


Research Article

The Impact of Microscopic Pore Network Characteristics on Movable Fluid Properties in Tight Oil Reservoir

Jie Gao ¹, Hu Wang,² Xiaojun Ding,³ Qingxiao Yuchi,⁴ Qiang Ren,⁵ Bo Ning,⁶ and Junxiang Nan⁷

¹School of Civil Engineering and Geodesy, Shaanxi College of Communication Technology, Xi'an 710018, China

²The Sixth Gas Production Plant, PetroChina Changqing Oilfield Company, Xi'an 710018, China

³Research Institute of Exploration and Development, PetroChina Qinghai Oilfield Company, Dunhuang 736202, China

⁴No. 12 Oil Production Plant, PetroChina Changqing Oilfield Company, Qingyang 745400, China

⁵School of Geology Engineering and Geomatics, Chang'an University, Xi'an 710054, China

⁶PetroChina Research Institute of Petroleum Exploration & Development, Beijing 100083, China

⁷Research Institute of Exploration and Development, PetroChina Changqing Oilfield Company, Xi'an 710018, China

Correspondence should be addressed to Jie Gao; 28372396@qq.com

Received 29 August 2022; Revised 30 September 2023; Accepted 13 October 2023; Published 14 November 2023

Academic Editor: Wenhui Li

Copyright © 2023 Jie Gao et al. This is an open access article distributed under the Creative Commons Attribution License, which permits unrestricted use, distribution, and reproduction in any medium, provided the original work is properly cited.

The fluid flow behavior, generally referred to as seepage, could determine the hydrocarbon and brine movement behavior. Movable fluid property, as one of the vital parameters for seepage characteristic evaluation, was generally used for tight oil reservoirs' fluid flow ability assessment. The nuclear magnetic resonance technique was used to experiment with movable fluid percentage and movable fluid porosity, which can provide a realistic assessment of the amount of fluid that can flow in the porous media. Other techniques were also used to analyze the main factors in regulating the differences in movable fluid parameters. However, the research about fluid flow behavior was generally based on traditional methods, while the seepage characteristics from the pore-scale view are still a myth. To promote this process, in this study, core samples obtained from the Chang 7 reservoir of the Triassic Yanchang Formation in the Longdong region of Ordos Basin, China, were tested. The results show that the average movable fluid percentage and average movable fluid porosity of the total 16 core samples are 36.01% and 2.77%, respectively. The movable fluid exists mainly in the midlarge pores with the corresponding T_2 relaxation time over 10 ms. T_2 distributions mainly present four typical patterns: (1) bimodal distribution with similar amplitudes of the two peaks (occupying 6.25%), (2) bimodal distribution with higher right peak and lower left peak (occupying 18.75%), (3) bimodal distribution with higher left peak and lower right peak (occupying 56.25%), and (4) unimodal distribution (occupying 18.75%). Pore structure heterogeneity is closely related to the movable fluid parameters; the movable fluid parameters exhibit a relatively good correlation with core throat radius as well as permeability. There is an obvious difference between the movable fluid parameters and the microscopic characteristic factors in tight oil reservoirs due to the difference in physical properties, clay mineral content, microcracks, and pore structure characteristics. This research has provided a new perspective for the movable fluid property evaluation, and the relevant results can give some advice for the oil field development.

1. Introduction

Tight oil reservoir is a typical unconventional oil resource, and it has become the new hot spot in global oil exploration and development in recent years [1, 2]. In China, the Chang 7 tight oil reservoir in the Longdong region of the Ordos Basin has been found to contain resource-rich tight oil in

recent years' investigation, which shows a good prospect in future exploration [3, 4]. However, due to technical limitations, tight oil reservoir studies are still at the primary stage [5]. It is shown that by the effects of deposition and diagenesis, the tight oil reservoir formed a large number and complex micro-nanometer pore throat during its development and also displayed a difference of movable fluid

occurrence distribution in tight oil reservoirs compared with low-permeability reservoirs, which led to a large change range in movable fluid parameter and a weak ability in fluid flow, resulting in an inappropriateness and difficulty in exploiting tight oil reservoirs [5–7].

Movable fluid parameters are effectively used in demonstrating the seepage characteristics and evaluating the potential capacity of tight oil reservoir exploration [8, 9]. Quantitative evaluation, distribution, and controlling factor analysis of movable fluid can accurately estimate the practicable resources for valuable exploration, which can also provide a theoretical basis for the development and adjustment of technological plans [10–12]. This study mainly used the nuclear magnetic resonance (NMR) relaxation technique and high-speed centrifugation system to investigate the microstructures of different tight oil reservoirs. In addition, thin section analysis (CTS), scanning electron microscopy (SEM), high-pressure mercury injection (HPMI), and high-resolution X-ray computerized tomography (CT) were also involved in describing the occurrence characteristic of movable fluid. Through this, an internal correlation between occurrence characteristics and geological factors was demonstrated in this paper, and thus, it can provide a scientific basis for Chang 7 tight oil reservoir exploration in the future.

2. Geological Background

Longdong area is located in the southwest of Ordos Basin, China, crossing the Yishan slope and the Tianhuan depression (Figure 1). The geological structural features of the Chang 7 segment are not complicated, which performed as a large monoclinic gentle slope from east to west with a lower dip angle [13]. Part of the regions presented a low-amplitude nose structure [13]. The lake transgression of Chang 7 reached its peak during the period of deposition, and the lake delta and gravity flow deposits were the main parts of the Chang 7 depositional system, while the favorable reservoir was sandy debris flow and distributary channel of the lake delta front [14, 15]. The thickness of the Chang 7 segment is 80–120 m [15]. For its lithology, the upper part is dark gray argillaceous siltstone mudstone, siltstone, and fine sandstone, while the lower part is dark gray mudstone, gray and black carbonaceous mudstone, and siltstone (Figure 1). The rock types are mainly lithic feldspathic sandstones and feldspathic rock fragment sandstones [14]. On average, there are 45.9% of quartz, 24.4% of feldspar, 28.4% of debris, and 1.3% of others, which indicates that the Chang 7 segment has a lower component of maturity [16–18]. In addition, the medium-strong compaction, diverse types of cementations, and common existing but not strong dissolution were the main forces during the lithology diagenesis [17]. The reservoir structure is midsmall pore and micro-fine throat type, and physical properties are poor, which indicates that Chang 7 is a typical low-porosity and ultra-low-permeability reservoir [19].

3. Materials and Methods

3.1. Sample Selection. Sample selection was based on the study of reservoir characteristics, also combined with the

investigation of interpretation, sedimentary sandy, and conventional physical properties. Therefore, 16 oil-bearing sandstone samples were selected from the Chang 7 reservoir, which were further used for NMR relaxation and high-speed centrifugal experiments. To investigate the microfactors that influenced the movable fluid occurrence characteristic, sample analysis was also carried out by physical property analysis, CTS, SEM, HPMI, and CT.

3.2. Instruments and Procedures. NMR relaxation experiments were performed with the low-field nuclear magnetic resonance analyzer, which is self-developed by the Institute of Seepage Fluid Mechanics, Chinese Academy of Sciences. The instrument has reached the internationally advanced level, and it can analyze various sizes of core with diameters less than 120 mm. The procedure is as below:

- (1) Drill 2.5 cm diameter plunger samples, and then, wash with the solvent (ethanol+benzene) to a cleanliness level lower than fluorescence level 3. After the samples were dried, measure the weight, length, diameters, and gas permeability. Vacuum samples over 12 hours, pressurize 12 MPa saturation water to simulate formation water, measure the wet weight, and calculate porosity
- (2) Place the 100% water-saturated core samples on the probe of the low magnetic field NMR analyzer, run the T_2 test, and inversely calculate the T_2 relaxation time spectrum. The main test parameters are 2.38 MHz of resonant frequency, 300 μ s of echo time, 3000 ms of waiting time, 1024 numbers of echoes, 64 numbers of scanning, and 50 of enhancement
- (3) Centrifuge the samples with 20 psi, 40 psi, 200 psi, and 400 psi, and follow with the NMR T_2 test as described in step (2)
- (4) Conduct CTS, SEM, HPMI, and CT tests

4. Results

4.1. Characteristics of Physical Properties. Table 1 illustrates the basic physical properties in Chang 7 formation. The results showed that porosity ranged from 5.42% to 9.89% with an average of 7.77%, and permeability is distributed between 0.0146 and $0.1543 \times 10^{-3} \mu\text{m}^2$, with an average of $0.0651 \times 10^{-3} \mu\text{m}^2$.

4.2. Characteristics of Movable Fluid Parameter. Table 1 also demonstrates the movable fluid parameters in Chang 7 formation. The results show that the distribution of movable fluid percentage was in the range of 7.23–60.29%, with an average of 36.01%, and the differential between maximum and minimum was 8.34. For movable fluid porosity, it was in the range of 0.12–6.11%, with an average of 2.77%, and the differential between maximum and minimum was 52.12%. These indicated that movable fluid parameters display a lower value and a larger difference of the tight oil reservoirs. The amplitude of variation of movable fluid porosity

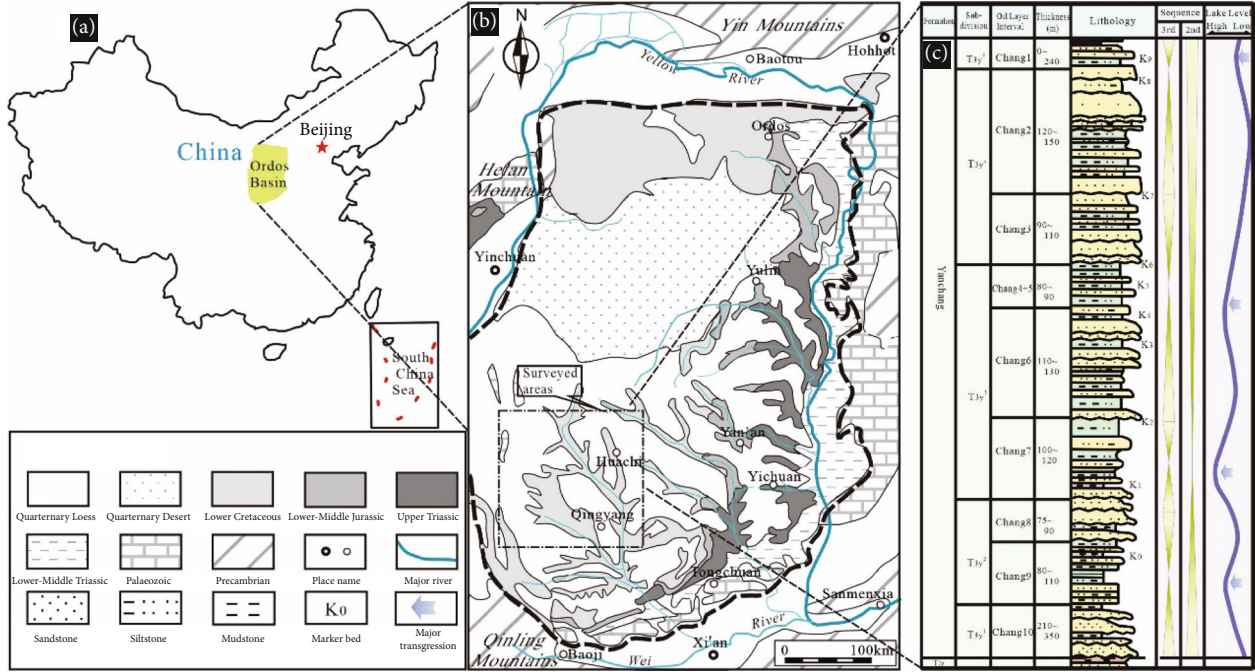


FIGURE 1: Map showing the location of the surveyed area of the Ordos Basin, China (modified from Ref. [14, 19]).

TABLE 1: Laboratory results of movable fluid from Chang 7 tight oil reservoir in Ordos Basin.

Well	Porosity (%)	Permeability ($\times 10^{-3} \mu\text{m}^2$)	Irreducible fluid percentage (%)	Movable fluid percentage (%)	Movable fluid porosity (%)
C7-1	8.97	0.1543	44.66	55.34	4.97
C7-21	9.89	0.0490	59.00	41.00	4.06
C7-22	7.54	0.0324	59.20	40.80	3.08
C7-3	7.24	0.0387	62.37	37.63	2.73
C7-4	6.86	0.0689	75.59	24.41	1.53
C7-5	5.42	0.0146	89.36	10.64	0.58

was much larger than the percentage of movable fluid, indicating a strong heterogeneous feature within samples.

T_2 spectrum data demonstrated that, for the different individual samples, the distribution of movable fluid was wide (Figure 2). As shown in Figure 2(b), the movable fluid of sample C7-3 existed in the T_2 relaxation time 3-1000 ms corresponding pores, while in Figure 2(c), the movable fluid of sample C7-2 existed in the 0.3-200 ms corresponding pores. Thus, these indicated that movable fluid did not only exist in large pores; most of them were reserved in the mid-large pores with the corresponding T_2 relaxation time over 10 ms, while there was also a small amount of movable fluid distributed in the tiny pores. On the contrary, bound fluid mainly existed in tiny pores. There were also amounts of bound fluid in the large pores; however, due to the complex features of Chang 7 tight oil reservoir, there were large amounts of dead pores or tiny pore throat that blocked mid-large pore throat, which led to weak connectivity within the pore throats, and the fluid seepage in large pores cannot occur under the centrifugal force; thus, NMR relaxation test demonstrated the bound fluid within these pore throats.

Therefore, bound fluid can exist in mid-large pores while movable fluid also can be detected in tiny pores; the distribution of movable fluid was wide.

4.3. NMR T_2 Spectrum Feature. NMR T_2 spectrum contains rich information on rock features. According to the different peak shapes, relaxation time, and amplitude, the T_2 spectrum can directly indicate the volume of movable fluid in different types of pores [20]. In our study, NMR T_2 spectrums of Chang 7 tight oil reservoir samples were mainly bimodal, either in different states of saturated formation water or under different centrifugal forces. The two peaks have differences in amplitude, and the spectrums also contain a certain amount of single peak form. NMR T_2 spectrums of samples that simulated saturated formation water can reflect the distribution of movable fluid in pore throats. As shown in our data, Chang 7 tight oil reservoirs have complex spectrum forms; T_2 distributions mainly present four typical patterns (Figure 2 and Table 2): (1) bimodal distribution with similar amplitudes of the two peaks (occupying 6.25%) (Figure 2(a)), (2) bimodal distribution with higher

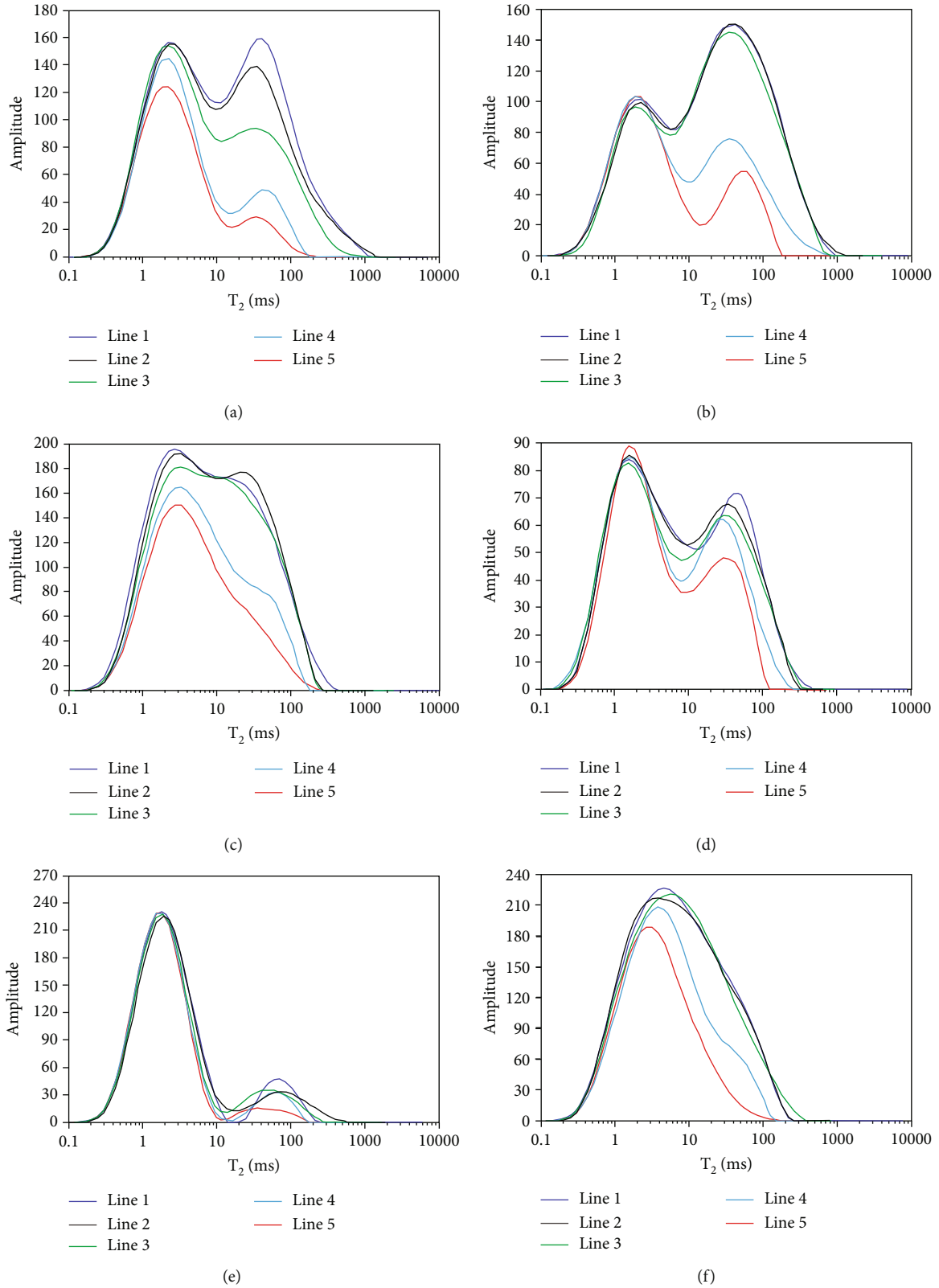


FIGURE 2: Representative NMR T_2 pattern of Chang 7 tight oil reservoir in Ordos Basin: (a) sample from well C7-1, 2190.3 m; (b) sample from well C7-3, 2224.9 m; (c) sample from well C7-21, 1782.8 m; (d) sample from well C7-4, 2409.2 m; (e) sample from well C7-5, 2243.0 m; (f) sample from well C7-22, 1775.2 m. Lines 1-5 represent water-saturated core samples, 20 psi, 40 psi, 200 psi, and 400 psi, respectively.

TABLE 2: Statistics of reservoir characteristic parameters from different T_2 spectrums of samples.

Well	Radius max of throat (μm)	Mainstream throat radius (μm)	Microcrack distribution	Clay content (%)	Movable fluid percentage (%)	Patterns of T_2 distribution
C7-1	1.168	0.464	Microcrack	13.6	57.8	STP
C7-3	0.816	0.254	/	13.0	53.5	HRP
C7-21	0.738	0.213	/	10.0	44.5	HLP
C7-4	0.511	0.153	/	16.0	25.4	HLP
C7-5	0.377	0.109	/	19.0	14.1	HLP
C7-22	0.563	0.093	Microcrack	9.0	40.8	UM

Note: STP, HRP, HLP, and UM represent similar amplitudes of the two peaks, higher right peak and lower left peak, higher left peak and lower right peak, and unimodal distribution, respectively.

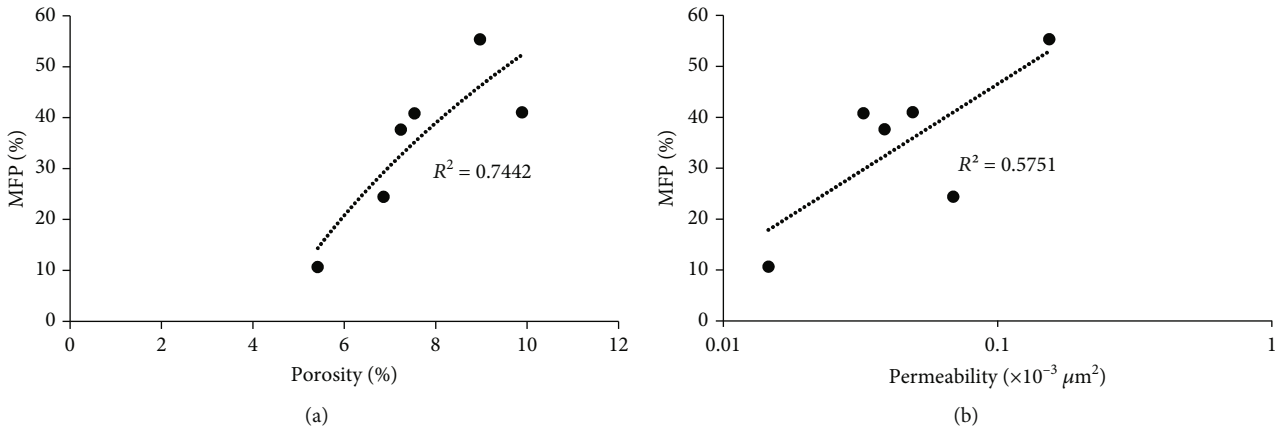


FIGURE 3: Relationship between movable fluid percentage and physical property. MFP: movable fluid percentage.

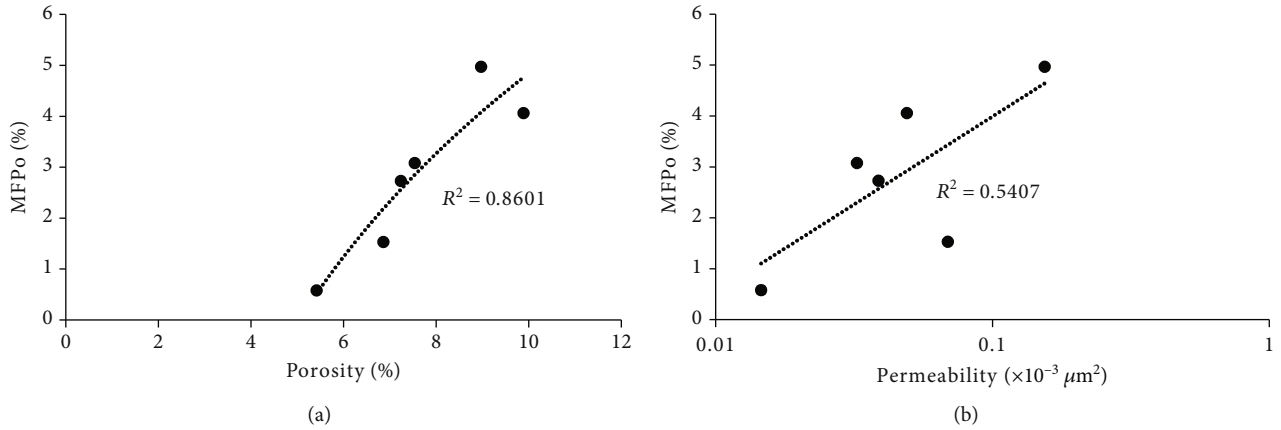


FIGURE 4: Relationship between movable fluid porosity and physical property. MFPO: movable fluid porosity.

right peak and lower left peak (occupying 18.75%) (Figure 2(b)), (3) bimodal distribution with higher left peak and lower right peak (occupying 56.25%) (Figures 2(c)–2(e)), and (4) unimodal distribution (occupying 18.75%) (Figure 2(f)). Therefore, within the maximum centrifugal force (400 psi) of the instrument, the distribution of sample NMR T_2 spectrums was mainly bimodal and unimodal.

The results indicated that the distributions of T_2 spectrums were mainly three types: right peak higher than left

peak, left peak higher than right peak, and single peak. The differences in T_2 spectrums among samples were mainly due to the microscopic features of reservoir parameters (Table 2). For instance, the sample with a higher left peak indicated that the reservoir has a poor property, small pore throat radius, high content of clay minerals, and undeveloped microfracture. However, the samples with higher right peaks or equal levels of peaks normally indicated that the reservoir has a good property, large pore throat radius, lower

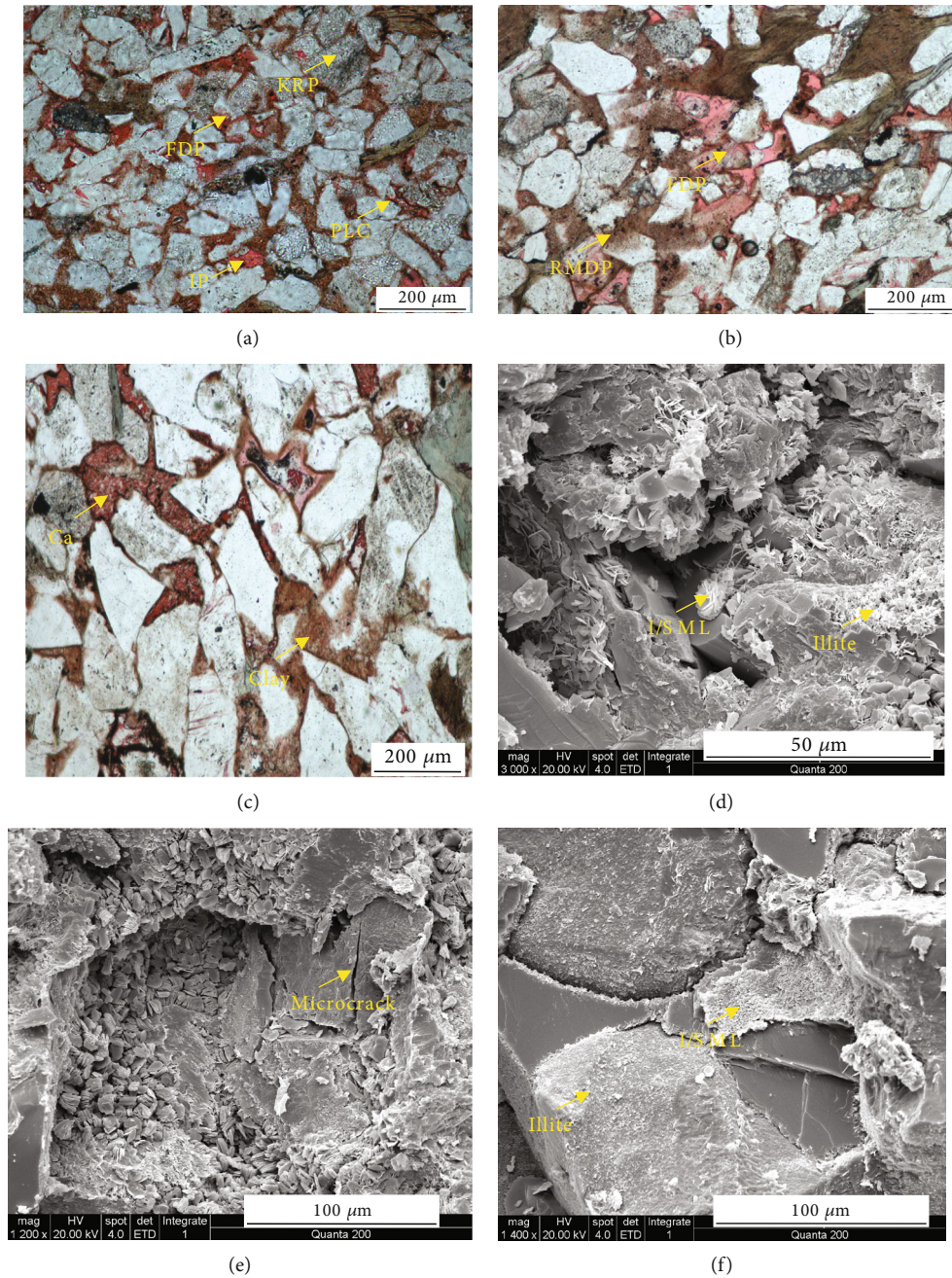


FIGURE 5: Typical pore types in research areas: (a) intergranular pores, feldspar dissolution pores, and kaolinite-related pores with pore-lining chlorite; (b) feldspar and rock matrix dissolution pores; (c) micropores related to calcite and clays; (d) feldspar dissolution pores with illite and I/S mixed layer; (e) microcracks; (f) illite, I/S mixed layer-related micropores. IP: intergranular pore; FDP: feldspar dissolution pore; KRP: kaolinite-related pore; PLC: pore-lining chlorite; RMDP: rock matrix dissolution pore; I/S ML: I/S mixed layer.

content of clay minerals, and well-developed microfractures. The samples with single peaks have intervenient microscopic features. Therefore, the differences in microscopic features of reservoirs led to diversified patterns of T_2 spectrums.

5. Discussion

The parameters of movable fluid in Chang 7 tight oil reservoirs showed a variety of differences among sample regions and depth. Chang 7 tight sandstone reservoir in Ordos Basin

has several features: poor properties, a large number of micro-nanometer pores throats, high interstitial content, and inartificial fractures. In addition, the level of throat developed and connected, the characteristics of clay minerals, and the fractures developed were the main factors in regulating movable fluid distribution.

5.1. Effect of Physical Properties. In this section, we analyzed the correlation between movable fluid parameters and the physical properties (Figure 3). The results showed that the

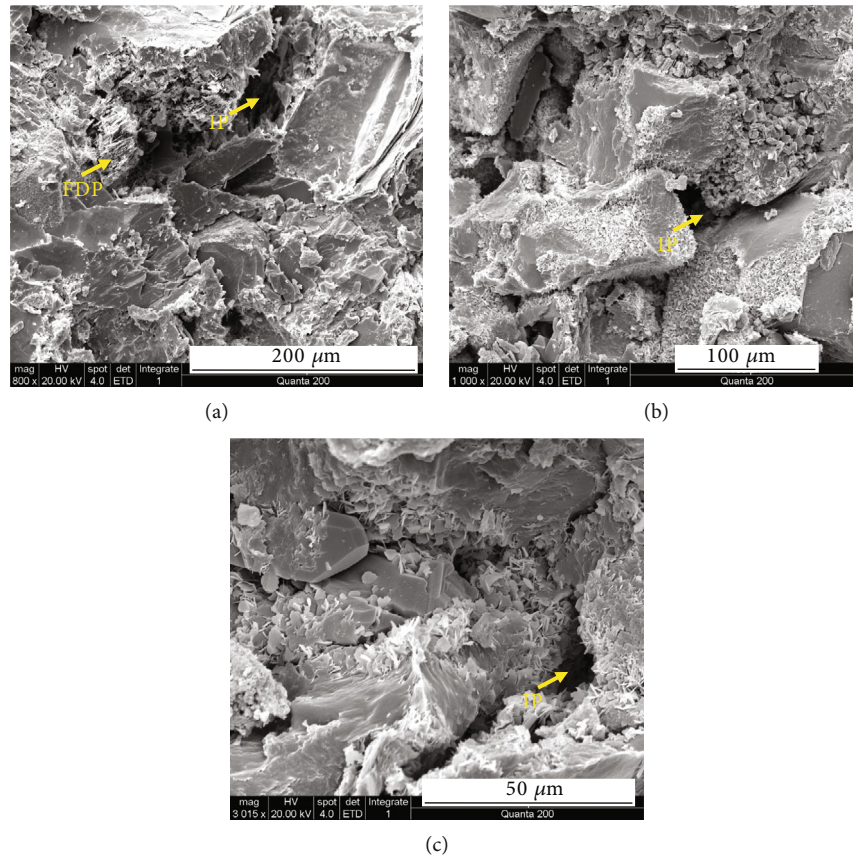


FIGURE 6: Scanning electron microscopy images of Chang 7 tight oil reservoir in Ordos Basin: (a) sample from well C7-1, 2185.2 m, intergranular pore and dissolution pore; (b) sample from well C7-3, 2225.1 m, intergranular pore; (c) sample from well C7-5, 2243.3 m, intergranular micropore. IP: intergranular pore; FDP: feldspar dissolution pore.

percentage of movable fluid in Chang 7 reservoirs has a weak correlation with porosity, while it has a relatively better correlation with permeability. The distribution of movable fluid percentage was relatively wide; with the increasing porosity and permeability, the data point tended to be decentralized. The reservoirs that have high porosity and permeability may not contain a high percentage of movable fluid, while the reservoirs that have low porosity or permeability showed a small difference in movable fluid percentage. For the reservoirs that have similar porosity and permeability, the percentage of movable fluid also contained a large difference. Therefore, in the case of weak properties of reservoirs, physical properties highly influenced the percentage of movable fluid; however, in the situation of better properties, the percentage of movable fluid was influenced by multiple factors and had a lower effect than physical properties displayed.

The porosities of movable fluid have a positive correlation with reservoir properties (Figure 4). Movable fluid porosity is the product of porosity and percentage of movable fluid. This parameter can comprehensively indicate the characteristics of movable fluid and porosity. Thus, the correlation of movable fluid porosity with porosity was better than the correlation of porosity with the percentage of movable fluid; in addition, with the increase of porosity, movable fluid porosity was greatly increased. Compared with the correlation of permeability with the percentage of

movable fluid, the correlation of permeability with movable fluid porosity was quite similar to each other. However, with the decrease of permeability, the decreasing amplitude of movable fluid porosity was reduced, while with the increase of permeability, the increasing amplitude of movable fluid porosity was rising.

5.2. Effects of Pore Structure. For the pore structures, there were several types of pores developed in Chang 7 tight sandstone reservoirs: residual intergranular pores, intergranular and intergranular dissolution pores, and intergranular pores. Among them, the content of dissolution pores was higher than the content of residual intergranular pores. Reservoir clastic particles were mainly in-line contact; the throats were mostly flakes, bent sheets, and tube-shaped; and those were sharply narrowed down. High-pressure mercury injection analysis displayed that the radius of throats was around 50 nm-300 nm, the reservoirs contained a high amount of fine pore throats and lower numbers of throat coordination, and the pore structure was complex. The correlation analysis of movable fluid parameters with pore throat structure parameters indicated that movable fluid parameters have a strong correlation with mainstream throat radius. Compared with the percentage of movable fluid, movable fluid porosity has a higher correlation with the mainstream throat radius. Throat radius affects the connectivity of reservoir

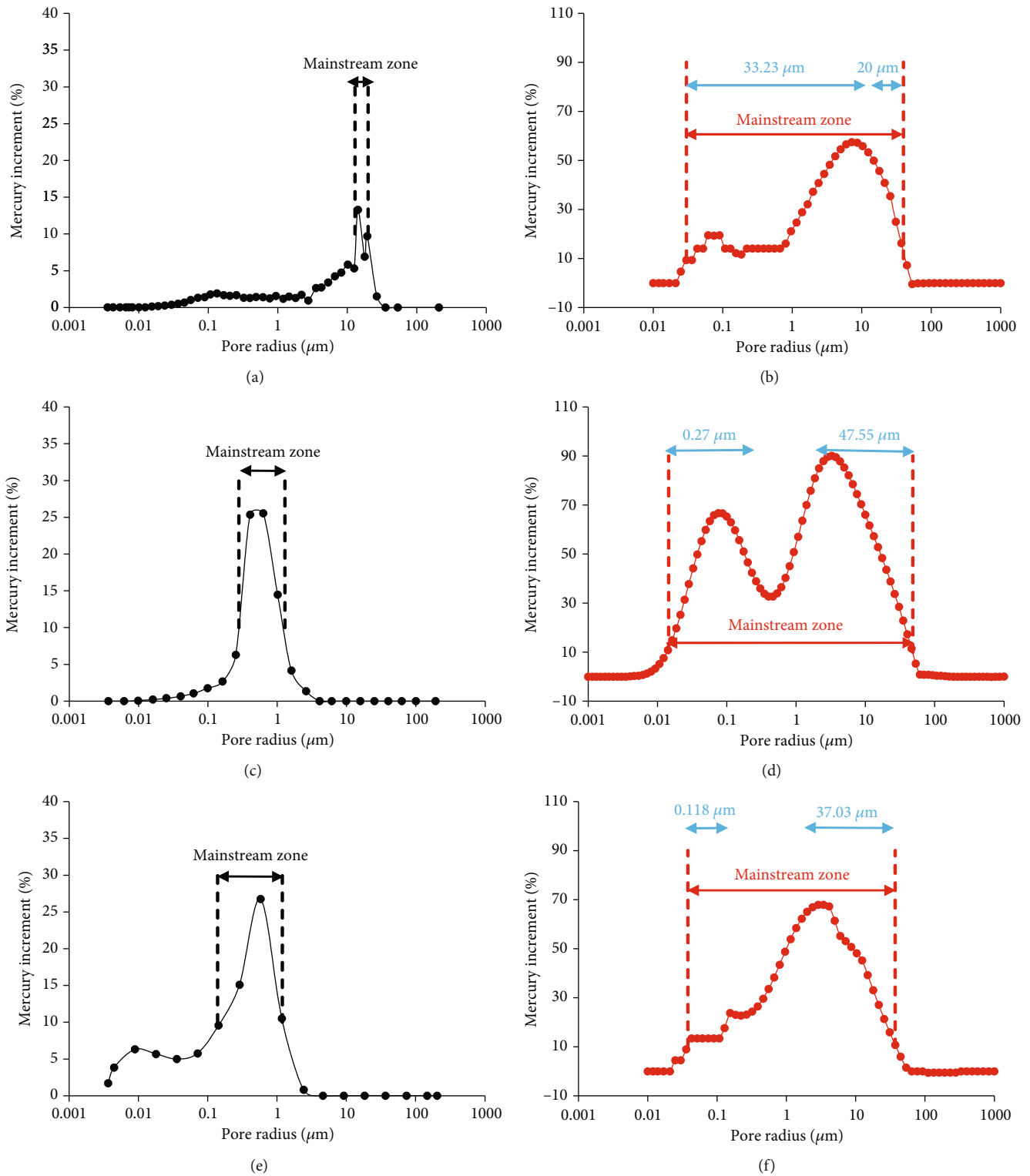


FIGURE 7: Continued.

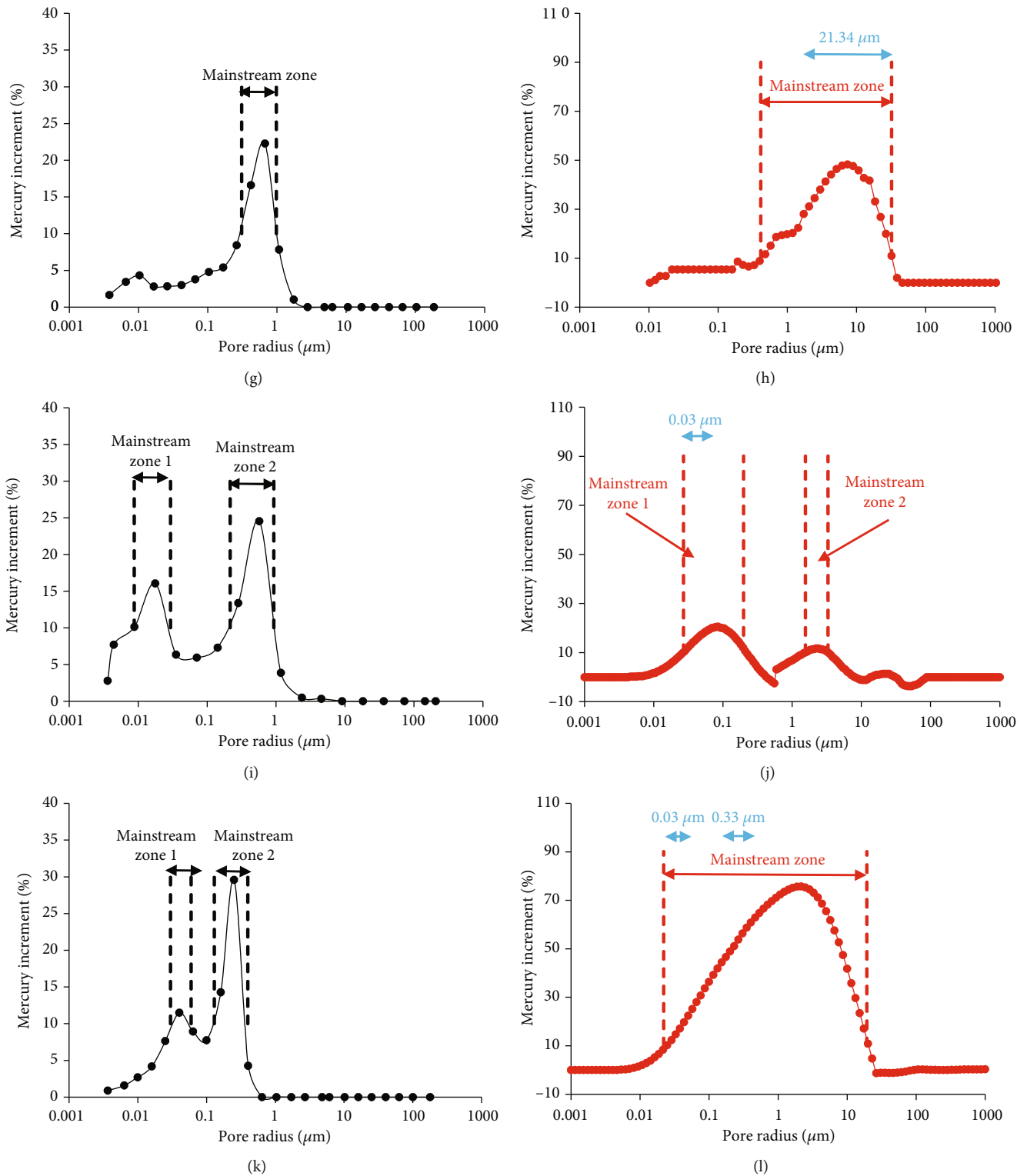


FIGURE 7: Pore radius distributions from HPMI and NMR data: (a) C7-1 from HPMI; (b) C7-1 from NMR; (c) C7-3 from HPMI; (d) C7-3 from NMR; (e) C7-21 from HPMI; (f) C7-21 from NMR; (g) C7-4 from HPMI; (h) C7-4 from NMR; (i) C7-5 from HPMI; (j) C7-5 from NMR; (k) C7-22 from HPMI; (l) C7-22 from NMR.

pores; it is easier for a larger radius of the pore throat to have fluid seepage occur, resulting in a strong effect of the throat radius that regulates the volume of movable fluid (Figure 5). The development of secondary porosity not only increased

the pore space of the reservoir but also enhanced the communication among different pores, which provided more flow channels for fluid flow and increased the reservoir movable fluid content. As shown in Figure 6(a), the residual

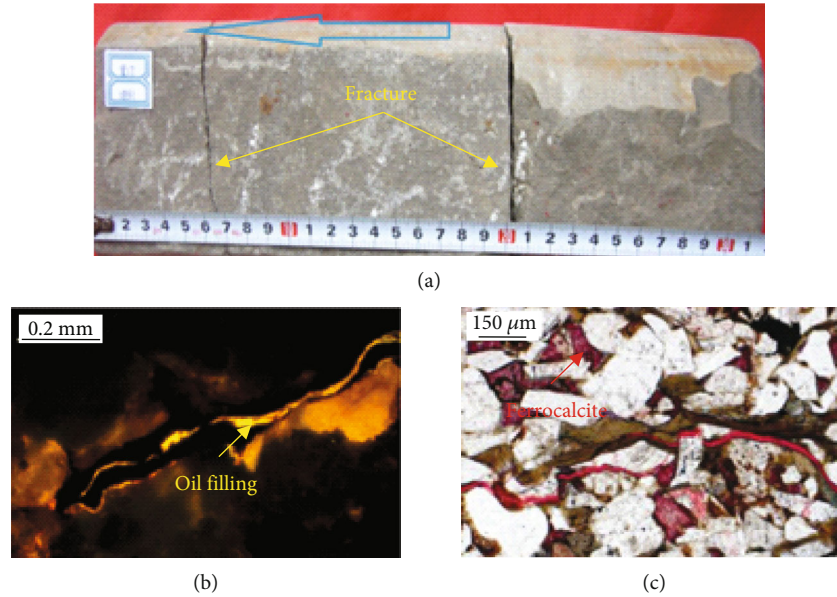


FIGURE 8: Fracture images of Chang 7 tight oil reservoir in Ordos Basin: (a) sample from well L17, 1831.2 m, high angle and unfilled fractures, oil stain; (b) sample from well F6, 1957.6 m, oil filling fracture; (c) sample from well X82, 2084.0 m, ferrocalcite filling pore, double fracture-pore system.

intergranular pores of the C7-1 sample were well developed, feldspathic dissolved pores were formed, the mainstream throat radius was around 430 nm, pore connectivity was good, and the movable fluid percentage was 53.63%. Sample C7-3 in Figure 6(b) showed the development of residual intergranular pores, secondary porosity was weak, the mainstream throat radius was around 287 nm, pore connectivity was good, and the movable fluid percentage was 32.32%. In sample C7-5 (Figure 6(c)), only a micropore was developed, the mainstream throat radius was around 109 nm, pore connectivity was poor, and the movable fluid percentage was only 14.05%.

Overall, the pore throat radius of the Chang 7 reservoir was small; pore connectivity was weak, which easily became dead pores; and the internal fluid became immobile fluid. This feature indicated that the content of reservoir movable fluid was strongly influenced by the pore structures, while the secondary porosity could increase the pore connectivity, which further increased the volume of movable fluid.

By combining the pore distribution obtained from HPMI experiments with the free water distribution obtained from NMR experiments, the influence of different pore structures on the properties of movable fluids can be clarified. As shown in Figure 7, the relationship between movable fluid and pore structure is evaluated by setting the mercury increment and movable fluid increment percentage above 10% as the main stream zone. The blue value indicates that the higher the saturation of the movable fluid, the more concentrated the range of the two types of mainstream zones and the larger the pore size difference between the main peaks. At the same time, for reservoirs with high mobile fluid saturation, the nonmain peak difference is generally divided into two sections: small aperture and large aperture. This indicates that the weaker the control ability of the main

peak of pore size on the movable fluid, the stronger the movement ability of the pore fluid. Homogeneity is a key pore structure factor controlling the saturation of the movable fluid.

5.3. Effects of Fractures. Natural fractures were widely developed in Chang 7 tight oil reservoirs. We investigated and calculated 54 wells of rock core in the basin. Among them, 31 wells contained different degrees of macrofractures, the drilling rate reached 57.4%, and 33.0% of fractures had a cutting depth over 50 cm. Among these 31 wells, there were 22 wells unfilled, the filling level of visible fractures was quite low, the developmental level of fractures was good, and efficiency was high. Reservoir fractures can increase the connectivity of pores and improve the flow capacity of tight reservoirs containing large amounts of movable fluid, which increases the volume of fluid and strongly influences the reservoir's movable fluid. As the sample in Figure 8(a), it contained a high angle and unfilled fractures. The fractures increased the connectivity and contained a large movable fluid flow space, which raised the total volume of movable fluid. Under the single polarizing microscope, sample fractures in Figure 8(b) have an obvious characteristic of oil immersion, which became the main occurrence space of movable fluid. The cast thin section showed that, in the sample of Figure 8(c), a large number of fractures were filled with iron calcite, and a minimal degree of pore developed, but the microfractures helped to increase the amount of movable fluid. Based on these, it indicated that the development level of fractures can improve the volume of reservoir movable fluid, even with a lower level of porosity and permeability. As the samples of well C7-1 (2188.1 m), porosity was around 6.55%, and permeability was $0.058 \times 10^{-3} \mu\text{m}^2$; however, with the X-CT scanning, it showed that multiple

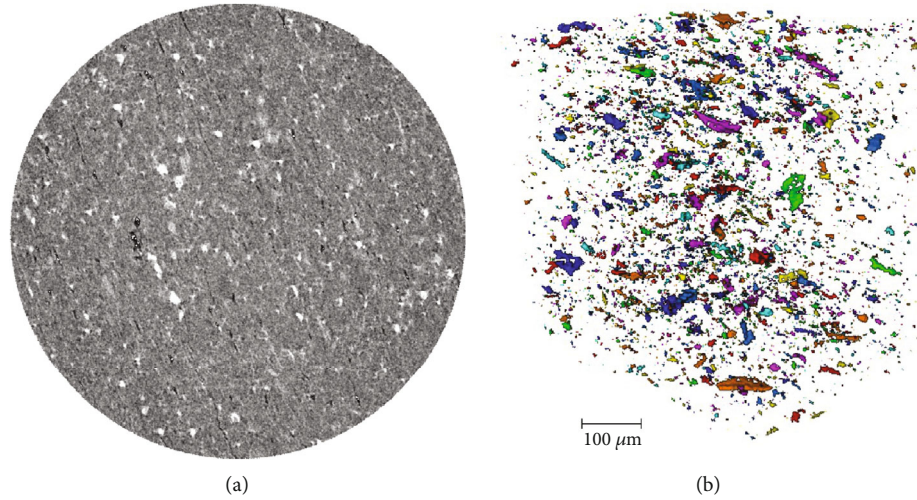


FIGURE 9: (a) Two- and (b) three-dimensional X-CT rock imageries of sample from well C7-1 (2188.1 m).

TABLE 3: X-diffraction clay mineral data table of Chang 7 tight oil reservoir in Ordos Basin.

Well	Relative clay mineral contents (%)				Absolute clay mineral contents (%)
	Kaolinite	Chlorite	Illite	I/S mixed layer	
C7-1	24.5	16.5	12.0	47.0	13.6
C7-3	22.3	14.5	19.8	43.4	13.0
C7-21	18.4	33.4	10.8	37.4	10.0
C7-4	21.4	20.5	25.2	32.9	16.0
C7-5	21.0	24.3	10.3	44.3	19.0
C7-22	20.0	46.0	8.0	26.0	9.0

fractures were developed in the sample (Figure 9), and the percentage of movable fluid reached to 49.6%. Therefore, microfractures can effectively increase the volume of movable fluid, and the different developmental degrees of microfractures could be the main reason for the difference of reservoir movable fluid in Chang 7 tight oil reservoirs.

5.4. Effects of Clay Minerals. Chang 7 reservoir contained a high content of interstitial, mainly kaolinite, chlorite, illite, illite mixed layer, and carbonates (mainly calcite and ankerite iron). The pore throat of reservoirs was filled with a high amount of interstitials, which damaged the reservoirs. The clay mineral composition, content, and occurrence of filled clastic particles strongly affected the volume of movable fluid. For Chang 7 reservoirs, clay minerals were mainly illite mixed layer, and the relative average content was 40.2%. Followed by chlorite, kaolinite, and illite, the average content was 26.8%, 20.8%, and 12.2%, respectively (Table 3). Sample pore throats were normally filled with clay minerals, and the filling degree was high, which led to a weak development and poor connectivity of pores. Movable fluids were influenced by different occurrences of clay minerals, curved sheets, or flocculent sheets of illite mixed layer, and illite was cut and filled in the primary intergranular pores, which led the pores to become tortuous. Furthermore, these effects seriously occurred in the narrow throats, which weakened the connectivity of pores and tended to the fluid flow into

bound fluid since the seepage was difficult. The lining chlorite is distributed on the surface of particles, it further narrowed the throats and reduced the efficiency of flow channels. Dispersed particles of kaolinite reduced the intergranular porosity, and it divided the porosity into fine pores, which increased the content of invalid pores. However, due to the nearly random distribution of kaolinite, it has little effect on the small volume of throats. Illite mixed layer and illite flakes have a greater influence on movable fluid while lining chlorite and dispersed particles of kaolinite have a relatively weak influence on movable fluid. Therefore, the content of clay minerals, occurrence types, and pore throat filling degrees strongly influenced the volume of movable fluid, and the movable fluid became bound fluid since it was difficult to flow. For instance, the sample of well C7-1 has a 5.51% of porosity, $0.015 \times 10^{-3} \mu\text{m}^2$ of permeability, 13.6% of absolute clay mineral content, and 32.3% of movable fluid percentage, kaolinite and chlorite-filled pore throat (Figure 10(a)). The sample of well C7-4 has a 6.42% of porosity, $0.070 \times 10^{-3} \mu\text{m}^2$ of permeability, 16% of absolute clay mineral content, and 25.4% of movable fluid percentage, illite mixed layer-filled pore throat (Figure 10(b)). The sample of well C7-5 has 9.23 % of porosity, $0.029 \times 10^{-3} \mu\text{m}^2$ of permeability, 19 % of absolute clay mineral content, and only 14.1 % of movable fluid percentage. For this sample, halite and illite mixed layer almost completely block the throat (Figure 10(c)).

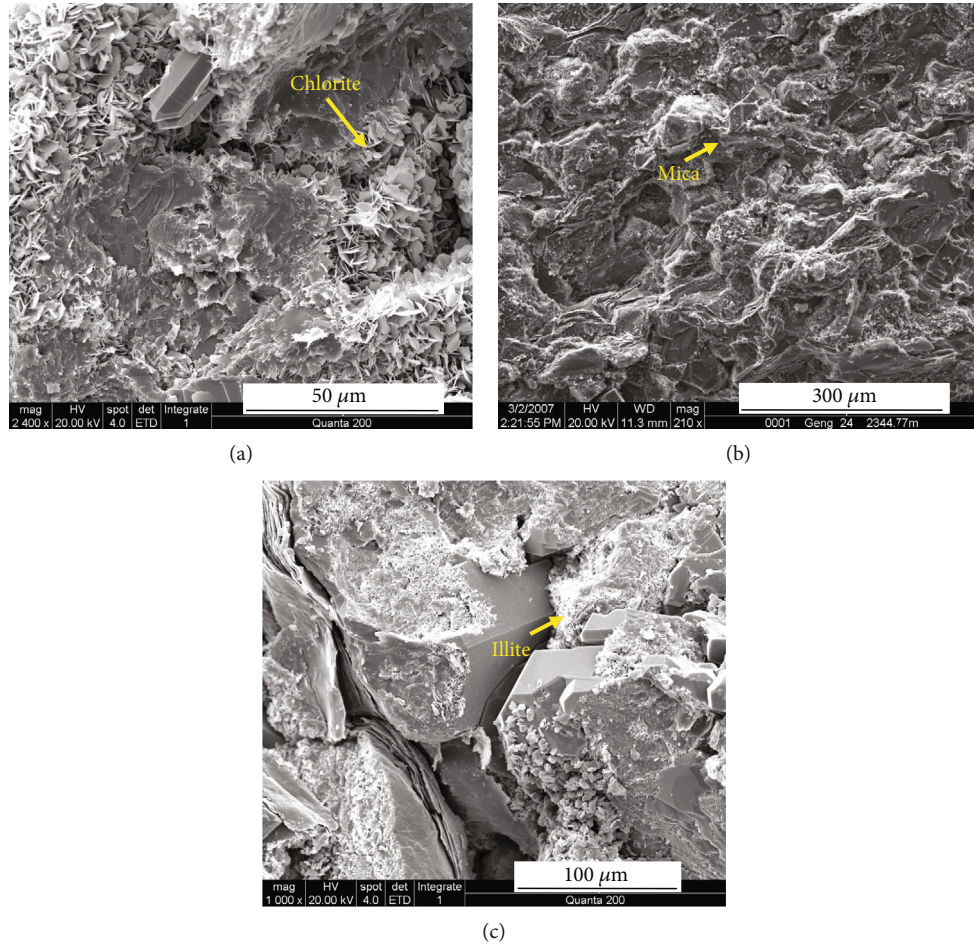


FIGURE 10: Scanning electron microscopy images of Chang 7 tight oil reservoir in Ordos Basin: (a) sample from well C7-3, 2225.9 m; (b) sample from well C7-4, 2409.2 m; (c) sample from well C7-5, 2243.0 m.

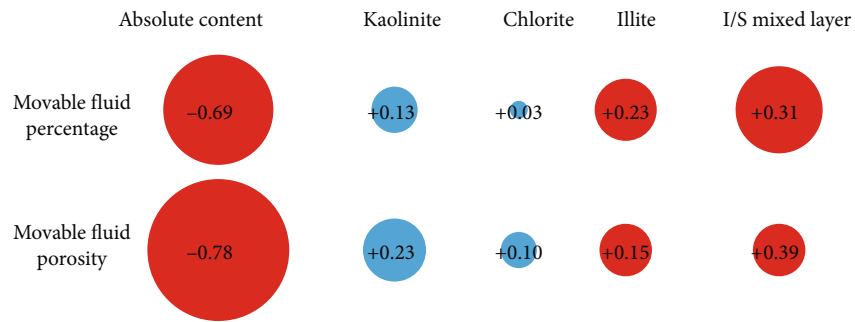


FIGURE 11: The relationship between the properties of movable fluids and the distribution of clay minerals.

Comparing the correlation between the content of clay minerals and the properties of movable fluids, it can be concluded that the higher the absolute content of clay minerals, the lower the saturation and porosity of movable fluids (Figure 11). The high content of kaolinite represents a certain degree of dissolution pores, which helps to increase the content of movable fluids. The relationship between chlorite and the properties of movable fluids is not significant.

Illite, especially the illite mixed layer, has a destructive effect on movable fluids. The high content of illite mixed layer leads to complex pore structure and affects the saturation of movable fluids. Overall, the porosity of movable fluids has a relatively significant impact on the content of clay minerals, indicating that clay minerals occupy the pores and have a much greater impact on the pore size of dense reservoirs than their absolute value.

6. Conclusion

- (1) With the lower physical properties, the changing range of movable fluid parameters was low. Movable fluid parameters showed a positive correlation with permeability
- (2) Movable fluid mainly existed in the large pores. However, there was a high amount of bound fluid in the midlarge pores, which led to a generally low parameter of movable fluid, the difference of parameters was quite high, and heterogeneity was strong
- (3) The distribution of microscopic reservoir pore throat radius, secondary throat porosity and connectivity, reservoir fracture occurrence and efficiency, clay mineral content and modes of occurrence, and the pore filling degree are the main factors for the different features of movable fluid distribution
- (4) The weaker the control ability of the main peak of pore size on the movable fluid, the stronger the movement ability of the pore fluid. Homogeneity is a key pore structure factor controlling the saturation of the movable fluid

Data Availability

The experimental data used to support the findings of this study are included in the manuscript.

Conflicts of Interest

The authors declare that there are no conflicts of interest regarding the publication of this paper.

Acknowledgments

This research was financially supported by the Shaanxi Natural Science Basic Research Program, China (No. 2021JM-543), the Major Project of Science and Technology of China (No. 2011ZX05044), the Innovation Project of Science and Technology of Shaanxi Province (No. 2015KTCL01-09), the China Postdoctoral Science Foundation (No. 2015M582699), and the Scientific Project from PetroChina Company (2021DJ2105). The authors greatly acknowledge Professor Weixi Sun from Northwest University (China) for useful discussions and comments on an earlier version of the manuscript.

References

- [1] J. Boak and R. Kleinberg, "Shale gas, tight oil, shale oil and hydraulic fracturing," in *Future Energy*, pp. 67–95, Elsevier, 2020.
- [2] M. Milad, R. Junin, A. Sidek, A. Imqam, and M. Tarhuni, "Huff-n-puff technology for enhanced oil recovery in shale/tight oil reservoirs: progress, gaps, and perspectives," *Energy & Fuels*, vol. 35, no. 21, pp. 17279–17333, 2021.
- [3] Y. Zhou, Y. Ji, L. Xu et al., "Controls on reservoir heterogeneity of tight sand oil reservoirs in Upper Triassic Yanchang Formation in Longdong area, southwest Ordos Basin, China: implications for reservoir quality prediction and oil accumulation," *Marine and Petroleum Geology*, vol. 78, pp. 110–135, 2016.
- [4] R. Guo, Q. Xie, X. Qu et al., "Fractal characteristics of pore-throat structure and permeability estimation of tight sandstone reservoirs: a case study of Chang 7 of the Upper Triassic Yanchang Formation in Longdong area, Ordos Basin, China," *Journal of Petroleum Science and Engineering*, vol. 184, article 106555, 2020.
- [5] F. I. Syed, A. K. Dahaghi, and T. Muther, "Laboratory to field scale assessment for EOR applicability in tight oil reservoirs," *Petroleum Science*, vol. 19, no. 5, pp. 2131–2149, 2022.
- [6] Y. Zhang and W. Guo, "Molecular insight into the tight oil mobility in nano-pore throat systems," *Fuel*, vol. 293, article 120428, 2021.
- [7] J. Qiao, J. Zeng, S. Jiang, and Y. Wang, "Impacts of sedimentology and diagenesis on pore structure and reservoir quality in tight oil sandstone reservoirs: implications for macroscopic and microscopic heterogeneities," *Marine and Petroleum Geology*, vol. 111, pp. 279–300, 2020.
- [8] D. Ren, X. Wang, Z. Kou et al., "Feasibility evaluation of CO₂ EOR and storage in tight oil reservoirs: a demonstration project in the Ordos Basin," *Fuel*, vol. 331, article 125652, 2023.
- [9] X. Kong, D. Xiao, S. Jiang, S. Lu, B. Sun, and J. Wang, "Application of the combination of high-pressure mercury injection and nuclear magnetic resonance to the classification and evaluation of tight sandstone reservoirs: a case study of the Linxing block in the Ordos Basin," *Natural Gas Industry B*, vol. 7, no. 5, pp. 433–442, 2020.
- [10] T. Hu, X. Pang, F. Jiang et al., "Movable oil content evaluation of lacustrine organic-rich shales: methods and a novel quantitative evaluation model," *Earth-Science Reviews*, vol. 214, article 103545, 2021.
- [11] C. Sun, H. Nie, W. Dang et al., "Shale gas exploration and development in China: current status, geological challenges, and future directions," *Energy & Fuels*, vol. 35, no. 8, pp. 6359–6379, 2021.
- [12] Y. Liu, L. Fan, W. Wang, Y. Gao, and J. He, "Failure analysis of damaged high-strength bolts under seismic action based on finite element method," *Buildings*, vol. 13, no. 3, p. 776, 2023.
- [13] C. Zou, S. Pan, B. Horsfield et al., "Oil retention and intrasource migration in the organic-rich lacustrine Chang 7 shale of the Upper Triassic Yanchang Formation, Ordos Basin, Central China," *AAPG Bulletin*, vol. 103, no. 11, pp. 2627–2663, 2019.
- [14] Y. Xuanjun, L. Senhu, L. Qun et al., "Lacustrine fine-grained sedimentary features and organic-rich shale distribution pattern: a case study of Chang 7 member of Triassic Yanchang Formation in Ordos Basin, NW China," *Petroleum Exploration and Development*, vol. 42, no. 1, pp. 37–47, 2015.
- [15] D. Li, R. Li, Z. Zhu et al., "Origin of organic matter and paleosedimentary environment reconstruction of the Triassic oil shale in Tongchuan City, southern Ordos Basin (China)," *Fuel*, vol. 208, pp. 223–235, 2017.
- [16] N. Sun, T. Chen, J. Zhong et al., "Petrographic and geochemical characteristics of deep-lacustrine organic-rich mudstone and shale of the Upper Triassic Chang 7 member in the southern Ordos Basin, northern China: implications for shale oil exploration," *Journal of Asian Earth Sciences*, vol. 227, article 105118, 2022.

- [17] H. Hou, L. Shao, Y. Li et al., “Effect of paleoclimate and paleo-environment on organic matter accumulation in lacustrine shale: constraints from lithofacies and element geochemistry in the northern Qaidam Basin, NW China,” *Journal of Petroleum Science and Engineering*, vol. 208, article 109350, 2022.
- [18] Y. Liu, D. Han, N. Liu, and W. Wang, “Reinforcement mechanism analysis of lattice beam and prestressed anchor rod system for loess slope,” *Frontiers in Earth Science*, vol. 11, article 1121172, 2023.
- [19] F. Tan, R. Zhao, Y. Zhao, Z. Pan, and H. Li, “A case study: evaluating low-porosity and ultra-low-permeability Triassic reservoir rocks in the Ordos Basin by the integration of logs and core,” *Petroleum Geoscience*, vol. 23, no. 4, pp. 454–465, 2017.
- [20] D. Liu, D. Ren, K. Du, Y. Qi, and F. Ye, “Impacts of mineral composition and pore structure on spontaneous imbibition in tight sandstone,” *Journal of Petroleum Science and Engineering*, vol. 201, article 108397, 2021.